Available online at www.sciencedirect.com
SCIENCE DIRECT®
Journal of Organometallic Chemistry 689 (2004) 917–929
Journal of Organometallic Chemistry
www.elsevier.com/locate/jorganchem

Synthesis and characterization of *N*-(2-pyridyl)benzamide-based nickel complexes and their activity for ethylene oligomerization

Wen-Hua Sun [a,*], Wen Zhang [a], Tielong Gao [a], Xiubo Tang [a], Liyi Chen [a], Yan Li [a], Xianglin Jin [b]

[a] *State Key Laboratory of Engineering Plastics and The Center for Molecular Sciences, Institute of Chemistry, Chinese Academy of Sciences, Zhongguancun, Beiyijie, Beijing 100080, China*
[b] *Institute of Physical Chemistry, Peking University, Beijing 100871, China*

Received 4 September 2003; accepted 16 December 2003

Abstract

A series of *N*-(2-pyridyl)benzamides (**1**)–(**11**) and their nickel complexes, [*N*-(2-pyridyl)benzamide]dinickel(II) di-μ-bromide dibromide (**12**)–(**16**) and (aryl)[*N*-(2-pyridyl)benzamido](triphenylphosphine)nickel(II) (**17**)–(**24**), were synthesized and characterized. The single-crystal X-ray analysis revealed that **12** and **14** are binuclear nickel complexes bridged by bromine atoms and each nickel atom adopts a distorted trigonal bipyramidal geometry. The key feature of the complexes **17**, **19** and **23** is each has a six-membered nickel chelate ring including a deprotonated secondary nitrogen atom and an O-donor atom. The nickel complexes show moderate to high catalytic activity for ethylene oligomerization with methylaluminoxane (MAO) as cocatalyst. The activity of **12**–**16**/MAO systems is up to 3.3×10^4 g mol^{-1} h^{-1} whereas for **17**–**24**/MAO systems it is up to 4.94×10^5 g mol^{-1} atm^{-1} h^{-1}. The influence of Al/Ni molar ratio, reaction temperature, reaction period and PPh_3/Ni molar ratio on catalytic activity was investigated.

Keywords: *N*-(2-Pyridyl)benzamide ligand; Nickel complexes; Crystal structures; Ethylene oligomerization

1. Introduction

The past decade has witnessed a significant progress in late-metal complexes for oligomerization and polymerization of olefins [1–6]. α-Diimine nickel/palladium complexes and bis(imino)pyridyl iron/cobalt complexes are the two kinds of well-known catalysts [7,8] used for oligomerization/polymerization of olefins. By tuning the steric and electronic properties of the active center, the catalytic products of the metal complexes differently suitable for polyethylene and oligomers [9–11] can be obtained. Recently, neutral nickel(II) complexes have attracted much attention because they are less sensitive to protonic solvents and polar monomers than cationic nickel analogues. The most famous example of neutral nickel(II) catalysts is the SHOP-type [12–18]. These nickel complexes contain an anionic [P, O] chelate ring and show high activity and selectivity for the conversion of ethylene to linear α-olefins and polymers. Neutral nickel(II) catalysts containing anionic [N, O] chelate ring were also largely reported in recent years [19–24]. One such type of catalyst is the neutral salicylaldimine nickel complex, reported by Grubbs' group, having the highest activity of 1.3×10^5 mol ethylene (mol Ni h)$^{-1}$ for ethylene polymerization [21]. In addition, other ligands such as phosphinooxazoline [25], dithio-β-diketonate [26], iminophosphine [27], monoiminopyridine [28], bis(pyrazolyl)methane [29], α-nitroketonate [30], bis(2-diphenylphosphinoethyl)methylamine [31], etc. have also been employed with late-metals as homogeneous catalysts.

In exploring new catalysts for ethylene activation in our laboratory, nickel complexes containing 8-aminoquinoline,

* Corresponding author. Tel.: +861062557955; fax: +861062618239.
E-mail address: whsun@iccas.ac.cn (W.-H. Sun).

0022-328X/$ - see front matter © 2004 Elsevier B.V. All rights reserved.
doi:10.1016/j.jorganchem.2003.12.022

2-(2-pyridyl)quinoxaline, 2,6-bis(imino)phenol, 2,9-bis-(imino)-1,10-phenathroline and hydrazone derivatives were investigated [32]. To the best of our knowledge, there is no report on using pyridylcarboxamide metal complexes for ethylene oligomerization. In this paper, *N*-(2-pyridyl)benzamides (**1**)–(**11**) and their two kinds of nickel complexes **12**–**24** were synthesized and characterized, and the catalytic properties of these complexes for ethylene oligomerization are reported.

2. Results and discussion

2.1. Synthesis and spectroscopic characterization

Compounds **1**–**11** were prepared in good yields through the condensation reaction of 2-aminopyridines and benzoic chloride or 4-nitrobenzoic chloride according to a modified procedure [33]. The reaction was smoothly performed in pyridine at room temperature. The resulting mixtures were quenched with water, filtered, and the white solid was thoroughly washed with water and dried in vacuum oven over night. ^{1}H NMR spectra and elemental analyses showed the products were pure enough for subsequent reactions.

The nickel complexes **12**–**16** were synthesized by mixing the THF solutions of (DME)$NiBr_2$ (DME = ethylene glycol dimethyl ether) and the corresponding ligands **1**–**5**, respectively (see Scheme 1). The resulting complexes were precipitated from reaction solutions after several minutes. They are all air-stable yellow to yellow-brown powders which can be easily recrystallized from acetone–ether solutions.

The neutral nickel complexes **17**–**24** were synthesized according to a reported method [21a]. When NaH was added to the THF solution of the corresponding ligand, many bubbles were produced immediately. The color of the resulting solution varied from colorless to orange according to the different substituents on the ligand. When dried in vacuo, the Na salt was combined with *trans*-[NiCl(Naph)$(PPh_3)_2$] or *trans*-[NiCl(Ph)$(PPh_3)_2$] in toluene. The mixture was stirred at room temperature for several hours resulting a clear solution. After filtration, concentration and precipitation by pentane, the crude product was obtained in satisfactory yield. Complexes **17**–**24** are all air-stable yellow to red powders and highly soluble in toluene, CH_2Cl_2 and $CHCl_3$, and insoluble in alkanes. The naphthyl-containing complexes **17**–**22** are very stable in solutions when exposed to air, but the phenyl-containing complexes **23**–**24** soon decomposed in solution after several hours.

In IR spectra of **1**–**5**, the weak and broad bands observed between 3183 and 3343 cm^{-1} are ascribed to the stretching vibration of N–H. The ^{1}H NMR spectra show a broad singlet peak in the range 8.05–8.65 ppm confirming the existence of the hydrogen of secondary amide. In IR spectra of the corresponding complexes **12**–**16**, the strong absorption bands in the range 1624 and 1636 cm^{-1} are ascribed to the C=O stretching vibration. However, these values are found to be higher field (1652–1677 cm^{-1}) for the original ligands **1**–**5**. The stretching vibration of pyridine ring at 1421–1459 cm^{-1} for **1**–**5** shifted to 1446–1461 cm^{-1} for their corresponding complexes **12**–**16**. This spectral data show that the nickel atom coordinates with the nitrogen atom of the pyridyl ring and the oxygen atom of the carbonyl group. In far infrared spectra of the complexes, the absorption bands between 123 and 95 cm^{-1} are ascribed to bridging Br–Ni stretching vibrations and bands between 237 and 185 cm^{-1} to terminal Br–Ni stretching vibrations [34]. These observations reveal that the complexes have a binuclear structure in solid state, which is confirmed by X-ray analysis of **12** and **14**.

In IR spectra of **17**–**24**, a group of strong bands appears in the range 1300–1600 cm^{-1} for the stretching vibration of aromatic rings, and there are no C=O stretching vibrations of the corresponding ligands in the range 1659–1691 cm^{-1}. In ^{31}P NMR spectra of naph-

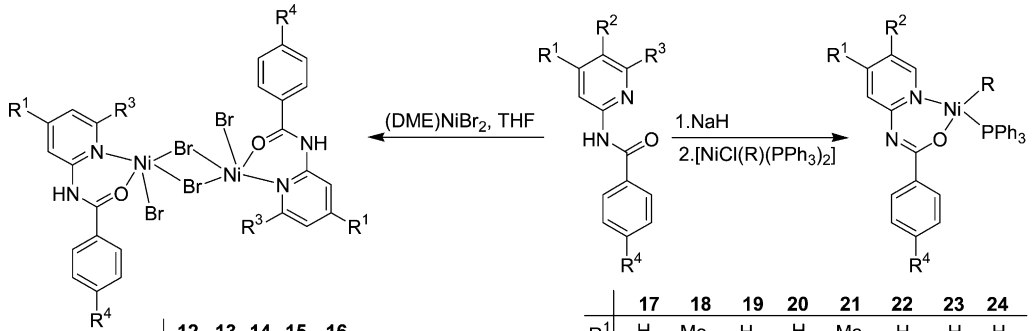

	12	13	14	15	16
R^1	H	Me	H	H	Me
R^3	Me	Me	Et	Me	Me
R^4	H	H	H	NO_2	NO_2

	17	18	19	20	21	22	23	24
R^1	H	Me	H	H	Me	H	H	H
R^2	H	H	NO_2	H	H	NO_2	NO_2	NO_2
R^4	H	H	H	NO_2	NO_2	NO_2	H	NO_2
R	Naph	Naph	Naph	Naph	Naph	Naph	Ph	Ph

Scheme 1. The synthesis of the nickel complexes **12**–**24**.

thyl-containing complexes **17**–**22**, the chemical shift of P atom is between 28.20 and 28.82 ppm compared to the value of 22.16 ppm of *trans*-[NiCl(Naph)(PPh_3)$_2$]. It is affected by the substituent on the pyridyl and phenyl rings of the ligand as shown in the following order: **19** < **17** < **18** and **22** < **20** < **21**. As to the phenyl-containing complexes **23**–**24**, the peak of P atom is at 29.22 and 29.45 ppm, respectively, a little higher than the values of **17**–**22**. The MALDI-TOF MS of **18** showed the most abundant peak at m/z 659.4, which is designated to the ionic molecule (m/z 659.2). This means the neutral nickel(II) complex is stable in organic solvents.

It is noteworthy that the *ortho*-alkyl substituent on the pyridyl ring in **1**–**11** played an important role for the formation of the desired nickel complexes. In the reaction of (DME)$NiBr_2$ and other *N*-(2-pyridyl)benzamide ligands (L) without alkyl substituent on the *ortho*-position of the pyridyl ring, L_2NiBr_2-type complexes were formed with a six-coordinate configuration around the nickel atom [35]. However, the expected neutral nickel complexes were not observed by using *N*-(2-pyridyl)benzamide ligands containing *ortho*-alkyl substituent on the pyridyl ring. The reason perhaps may be the adjacent steric interference between the *ortho* substituent and the R group (naphthyl or phenyl).

2.2. Crystal structure

Single crystals of **12** and **14** suitable for X-ray analysis were obtained by slow diffusion of ethyl ether into their acetone solutions. The structure of **12** shows a centro symmetric dinuclear nickel center (Fig. 1). Each nickel atom is coordinated by two atoms (O(1) and N(1)) of the ligand, one terminal bromine atom (Br(2)) and two bridging bromine atoms (Br(1) and Br(1A)). The bond lengths of Ni(1)–O(1), Ni(1)–N(1), Ni(1)–Br(1), Ni(1)–Br(2) and Ni(1)–Br(1A) are 1.944(3), 2.029(4), 2.587(1), 2.489(1) and 2.471(1) Å, respectively (Table 1). The nickel atom adopts a slightly distorted

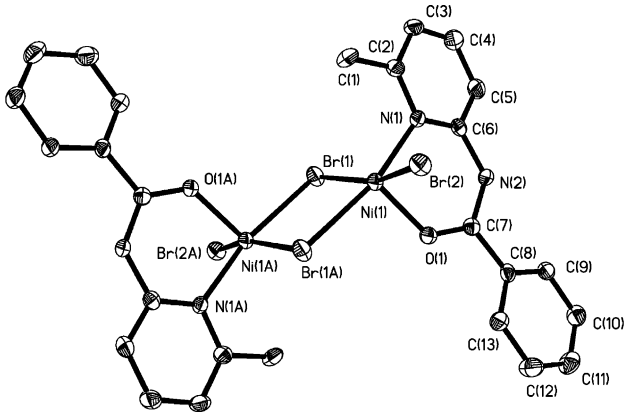

Fig. 1. Molecular structure of **12**, showing 30% probability displacement ellipsoids with hydrogen atoms omitted for clarity.

Table 1
Selected bond lengths (Å) and angles (°) for **12** and **14**

Complex **12**		Complex **14**	
Bond lengths			
Ni(1)–Br(1)	2.5874(12)	Ni(1)–Br(1)	2.4379(15)
Ni(1)–Br(2)	2.4887(10)	Ni(1)–Br(20)	2.4744(17)
Ni(1)–O(1)	1.944(3)	Ni(1)–O(1)	1.934(6)
Ni(1)–N(1)	2.029(4)	Ni(1)–N(2)	1.991(6)
Ni(1)–Br(1A)	2.4708(10)	Ni(1)–Br(1A)	2.5700(17)
Bond angles			
Ni(1)–Br(1)–Ni(1A)	95.21(3)	Ni(1)–Br(1)–Ni(1A)	95.00(5)
O(1)–Ni(1)–N(1)	91.75(13)	O(1)–Ni(1)–N(2)	93.1(3)
O(1)–Ni(1)–Br(1A)	97.76(9)	O(1)–Ni(1)–Br(1)	104.67(17)
N(1)–Ni(1)–Br(1A)	167.35(11)	N(2)–Ni(1)–Br(1)	160.64(19)
O(1)–Ni(1)–Br(1)	98.68(11)	O(1)–Ni(1)–Br(1A)	92.8(2)
N(1)–Ni(1)–Br(1)	85.55(11)	N(2)–Ni(1)–Br(1A)	86.54(19)
Br(1)–Ni(1)–Br(1A)	84.79(3)	Br(1)–Ni(1)–Br(1A)	85.00(5)
Br(2)–Ni(1)–Br(1)	163.22(3)	Br(2)–Ni(1)–Br(1A)	171.05(6)

Symmetry transformation used to generate equivalent atoms: A $-x, -y, -z$ for **12**; $-x, -y+2, -z$ for **14**.

trigonal bipyramidal geometry, in which the equatorial plane contains O(1), Br(1) and Br(2) atoms while the other two atoms (N(1) and Br(1A)) occupy the axial positions. The angle of N(1)–Ni(1)–Br(1A) is 167.35(11)° (smaller than 180°), and the Ni(1) atom locates 0.0163 Å above the equatorial plane toward Br(1A). The six-membered chelating ring of Ni(1)–N(1)–C(6)–N(2)–C(7)–O(1) is a distorted hexagon where the bond angle of O(1)–Ni(1)–N(1) is 91.75(13)°. The largest deviation of the plane is 0.0957 Å for C(6). The intramolecular distance of Ni–Ni is 3.736 Å, which is longer than the value of 3.686 Å observed in other dinickel complexes [36]. The ligand is nearly perpendicular to the Br(1)–N(1)–Br(2)–Br(1A) plane with a dihedral angle of 92.4°.

Complex **14** has a similar structure to its analogue **12**. The bond lengths of Ni(1)–O(1), Ni(1)–N(2), Ni(1)–Br(1), Ni(1)–Br(1A) and Ni(1)–Br(2) vary in the range 1.934(6)–2.570(2) Å. The nickel atom locates 0.0011 Å above the equatorial plane of O(1), Br(1A) and Br(2), toward Br(1). The bond angle of O(1)–Ni(1)–N(2) is 93.1(3)° in the six-membered chelating ring of Ni(1)–N(2)–C(8)–N(1)–C(7)–O(1). The intramolecular distance of Ni–Ni is 3.693 Å, which is 0.043 Å shorter than that in **12**. These differences between the two complexes derive from the different *ortho*-alkyl substituent of the pyridyl ring of them, i.e., ethyl group in **14** and methyl group in **12**.

In addition, hydrogen bonds are observed between terminal bromine atom and hydrogen atom of the secondary amide in the solid state of **12** and **14**. The 1-D chain diagram of **12** is shown in Fig. 2. In **12**, the hydrogen bond angle of N(2)–H(21)···Br(2#) (#: $-x, -y, 1-z$) is 164(4)°. The distance of H···Br is 2.60(5) Å and N(H)···Br is 3.560(4) Å. In **14**, the hydrogen bond angle of N(1)–H(15)···Br(2#) (#: $-x, 2-y, -1-z$) is 160(11)°. The distance of H···Br is

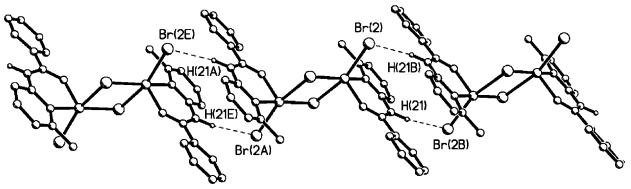

Fig. 2. The 1-D chain of **12**.

2.81(10) Å and N(H)···Br is 3.575(7) Å. The interaction of hydrogen bonds between the two neighboring molecules forms a 1-D infinite chain in the solid state structures of **12** and **14**.

Single crystals of **17**, **19** and **23** suitable for X-ray analysis were obtained by slow diffusion of pentane into toluene solutions. The structures of **17** and **23** are shown in Figs. 3 and 4, respectively. The selected bond lengths and angles are listed in Table 2.

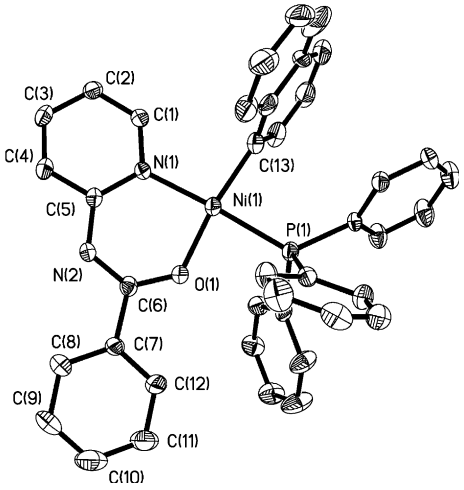

Fig. 3. Molecular structure of **17**, showing 15% probability displacement ellipsoids with hydrogen atoms omitted for clarity.

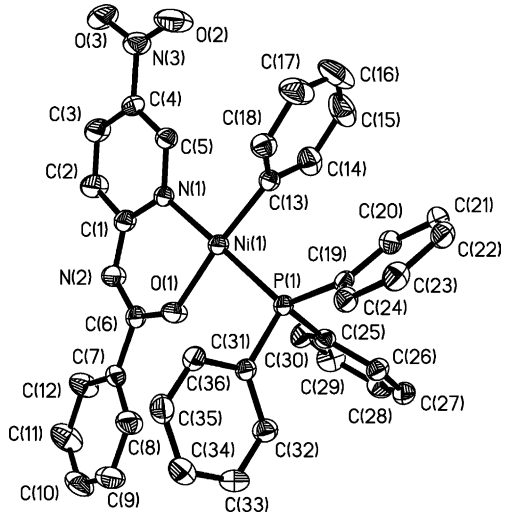

Fig. 4. Molecular structure of **23**, showing 30% probability displacement ellipsoids with hydrogen atoms omitted for clarity.

In **17**, the nickel center adopts a square planar geometry. The PPh_3 ligand takes the *trans* position to the nitrogen atom of the pyridyl ring. The bond lengths of Ni(1)–O(1), Ni(1)–N(1), Ni(1)–C(13) are found to be similar with a value of 1.9 Å while the Ni(1)–P(1) length is 2.191(2) Å. The pyridyl ring is nearly perpendicular to the naphthyl ring with a dihedral angle of 81.3°. Obviously the repulsion between the two rings and the bulkiness of the PPh_3 ligand enlarge the bond angle of C(13)–Ni(1)–N(1) to 95.26(18)° and reduce the bond angles of O(1)–Ni(1)–P(1) and C(13)–Ni(1)–P(1) to 84.69(9)° and 87.90(14)°, respectively. The bond lengths of O(1)–C(6), N(2)–C(6) and N(2)–C(5) are 1.275(4), 1.299(4) and 1.366(5) Å, respectively. They are shorter than the typical single bond lengths (C–O 1.36 Å and C–N 1.45 Å) but longer than the typical double bond lengths (C=O 1.22 Å and C=N 1.27 Å). It means that after the deprotonation of the ligand, the electron on the amide nitrogen partly delocalizes on the chelate ring O(1)–C(6)–N(2)–C(5)–N(1).

19 has a similar structure as **17**, but the existence of the nitro group on the 5-position of the pyridyl ring exerts some influence on the bond lengths and angles. The dihedral angle of the pyridyl ring and the naphthyl ring is 100.3°, which is higher compared to the value of **17**. The bond angle of C(13)–Ni(1)–N(1) increases a little to 96.6(4)° while the values of O(1)–Ni(1)–P(1) and C(13)–Ni(1)–P(1) are nearly equal (86.6(2)° and 86.3(3)°). The bond lengths of O(1)–C(6), N(2)–C(6) and N(2)–C(1) of the chelate ring O(1)–C(6)–N(2)–C(5)–N(1) are 1.240(8), 1.324(9) and 1.336(9) Å. The little difference of the bond lengths between O(1)–C(6) and O=C shows that the double bond is largely kept between O(1) and C(6).

As to **23**, the bond lengths between the nickel center and coordination atoms change little compared to **17** and **19**. The dihedral angle between the pyridyl ring and the phenyl ring is 99.9°. The repulsion between the two rings is less than that in **17** and **19**, i.e., the bond angle of C(13)–Ni(1)–N(1) changes to 93.75(9)° and the bond angles of O(1)–Ni(1)–P(1) and C(13)–Ni(1)–P(1) change to 86.24(5)° and 88.51(7)°, respectively. The bond lengths of O(1)–C(6), N(2)–C(6) and N(2)–C(1) are 1.269(3), 1.314(3) and 1.347(3) Å, respectively. Similar to **17** and **19**, the electron on the amide nitrogen of **23** partly delocalizes on the chelate ring O(1)–C(6)–N(2)–C(1)–N(1).

2.3. Mass spectroscopy

Although the solid state structures of **12**–**16** were confirmed by IR spectra and X-ray analysis, it is not clear what kind of species really exist in solution. The relatively weak interactions of the carbonyl oxygen atom and the bridging bromine atoms with the nickel atom would be somewhat destroyed by the solvents.

Table 2
Selected bond lengths (Å) and angles (°) for complex **17**, **19** and **23**

Complex **17**		Complex **19**		Complex **23**	
Bond lengths					
Ni(1)–O(1)	1.865(3)	Ni(1)–O(1)	1.874(5)	Ni(1)–O(1)	1.888(2)
Ni(1)–C(13)	1.938(6)	Ni(1)–C(13)	1.951(13)	Ni(1)–C(13)	1.887(2)
Ni(1)–N(1)	1.951(3)	Ni(1)–N(1)	1.976(6)	Ni(1)–N(1)	1.974(2)
Ni(1)–P(1)	2.1908(15)	Ni(1)–P(1)	2.189(2)	Ni(1)–P(1)	2.1816(8)
O(1)–C(6)	1.275(4)	O(1)–C(6)	1.240(8)	O(1)–C(6)	1.269(3)
N(2)–C(6)	1.299(4)	N(2)–C(6)	1.324(9)	N(2)–C(6)	1.314(3)
N(2)–C(5)	1.366(5)	N(2)–C(1)	1.336(9)	N(2)–C(1)	1.347(3)
Bond angles					
O(1)–Ni(1)–C(13)	171.6(2)	O(1)–Ni(1)–C(13)	172.4(4)	O(1)–Ni(1)–C(13)	174.57(9)
O(1)–Ni(1)–N(1)	92.10(13)	O(1)–Ni(1)–N(1)	90.5(3)	O(1)–Ni(1)–N(1)	91.37(8)
C(13)–Ni(1)–N(1)	95.26(18)	C(13)–Ni(1)–N(1)	96.6(4)	C(13)–Ni(1)–N(1)	93.75(9)
O(1)–Ni(1)–P(1)	84.69(9)	O(1)–Ni(1)–P(1)	86.63(17)	O(1)–Ni(1)–P(1)	86.24(5)
C(13)–Ni(1)–P(1)	87.90(14)	C(13)–Ni(1)–P(1)	86.3(3)	C(13)–Ni(1)–P(1)	88.51(7)
N(1)–Ni(1)–P(1)	176.74(12)	N(1)–Ni(1)–P(1)	177.0(3)	N(1)–Ni(1)–P(1)	174.71(6)
C(6)–N(2)–C(5)	124.2(3)	C(6)–N(2)–C(1)	120.7(7)	C(6)–N(2)–C(1)	123.9(2)
O(1)–C(6)–N(2)	126.6(4)	O(1)–C(6)–N(2)	128.1(8)	O(1)–C(6)–N(2)	127.5(2)

Mass spectroscopy of **12** in methanol and acetone were studied. The results are presented in Table 3.

From the ESI-MS values of the methanol solution of **12** ($[L_2Ni_2Br_4]$), it is clearly evident that the relative abundance of the binuclear species ($[L_2Ni_2Br_3]^+$) is as low as 5%. The mononuclear species ($[LNiBr]^+$) and its methanol adduct ($[LNiBr + CH_3OH]^+$) also have low abundance with the values of 5% and 10%. The most abundant species is the protonated ligand ($[L + H]^+$), indicating the decomposition of the complex. $[L_2NiBr]^+$ and $[L_2Ni–H]^+$ have high abundance (48% and 80%) in methanol, suggesting that the $[L_2NiBr_2]$ species is formed in the course. The MALDI-TOF-MS of **12** revealed a different map of the species existing in acetone. The strongest peak of the species is at m/z 619.4, which is ascribed to $[L_2NiBr + CH_3COCH_3]^+$ (calc. m/z 621.1). There is no sign of the protonated ligand ($[L + H]^+$).

Owing to the insolubility of **12** in toluene, we could not get a full knowledge of the real species of the complex in toluene when performing ethylene oligomerization. But the MS of **12** in polar solutions help us draw a conclusion that the ligand would coordinate nickel atom rather tightly and the binuclear species would be decomposed into mononuclear species in a large degree.

2.4. Ethylene oligomerization

2.4.1. Catalytic activity and oligomer distribution

The influence of cocatalyst MAO on catalytic activities and the distribution of resulting oligomers of **12**–**24** were carefully investigated. The results are summarized in Table 4.

Most complexes show good activity in the Al/Ni molar ratio of 300–1000. **18** showed the highest catalytic activity of 4.94×10^5 g mol^{-1} atm^{-1} h^{-1} at the Al/Ni molar ratio of 1000 at 22 °C. Reaction temperature exerted great influence on catalytic activities of **12**–**24**. Optimal catalytic activities were observed between 18 and 40 °C.

The change of ligands also clearly affects the activity of the corresponding complexes, i.e., the additional alkyl substituents on the pyridine ring impaired the catalytic activity for ethylene oligomerization. Under the mild catalytic conditions (Al/Ni 500, reaction temperature 18 °C), **14** with 6-ethyl group on pyridyl ring showed a catalytic activity of 3.3×10^4 g mol^{-1} h^{-1} while **13** with 4,6-dimethyl groups on pyridyl ring showed a relatively lower value of 1.3×10^4 g mol^{-1} h^{-1}. **15** and **16** containing NO_2-substituent on pyridine ring show relatively

Table 3
MS-species of **12** in methanol and acetone

Complex **12**[a] (methanol)	m/z Calc. (found)	Abundance (%)	Complex **12**[b] (acetone)	m/z Calc. (found)	Abundance (%)
$[L_2Ni_2Br_3]^+$	780.8 (781.0)	5	$[L_2Ni_2Br_3]^+$	780.8 (781.2)	9
$[L_2NiBr]^+$	563.0 (563.2)	48	$[L_2Ni_2Br_2–H]^+$	701.9 (702.2)	10
$[L_2Ni–H]^+$	481.1 (481.3)	80	$[L_2NiBr + CH_3COCH_3]^+$	621.1 (619.4)	100
$[LNiBr + CH_3OH]^+$	383.0 (383.1)	10	$[LNiBr_3]^+$	510.8 (510.6)	21
$[LNiBr]^+$	350.9 (351.1)	5	$[L_2Ni_2Br_3]^{2+}$	390.4 (389.2)	16
$[L_2Ni]^{2+}$	241.1 (241.2)	80			
$[L + H]^+$	213.1 (213.2)	100			

[a] ESI-MS.
[b] MALDI-TOF-MS.

Table 4
Ethylene oligomerization using **12**–**24**/MAO systems and their oligomers' distribution

Entry	Complex[a]	Al/Ni (mol/mol)	Temp (°C)	Activity (10^4 g mol^{-1} h^{-1})	Distribution of oligomers (%)[b]	
					C_4	C_6
1	**12**	500	18	2.0	78	22
2	**13**	300	18	1.3	93	7
3	**14**	100	18	3.8	83	17
4	**14**	300	18	3.9	83	17
5	**14**	500	18	3.3	84	16
6	**14**	1000	18	4.6	76	24
7	**14**	2000	18	2.9	83	17
8	**14**	500	0	0.7	88	12
9	**14**	500	40	1.2	80	20
10	**14**	500	60	0.8	84	16
11	**15**	300	18	3.1	86	14
12	**16**	1000	18	2.1	86	14
13	**17**	1000	40	33.3	84	16
14	**18**	100	22	0.8	93	7
15	**18**	300	22	10.9	92	8
16	**18**	500	22	41.9	88	12
17	**18**	1000	22	49.4	88	12
18	**18**	1500	22	36.2	87	13
19	**18**	2000	22	23.9	90	10
20	**18**	1000	0	16.7	97	3
21	**18**	1000	40	33.7	83	17
22	**18**	1000	60	21.3	76	24
23	**18**	1000	80	7.4	82	18
24	**19**	300	23	22.3	92	8
25	**20**	500	24	20.9	90	10
26	**21**	1000	24	35.7	88	12
27	**22**	2000	25	18.8	86	14
28	**23**	1000	28	22.3	85	15
29	**24**	1000	28	20.8	86	14

[a] Reaction condition: entry 1–12: 5 μmol catalyst, 40 ml toluene, 1 h, 1 atm ethylene; entry 13–29: 5 μmol catalyst, 30 ml toluene, 0.5 h, 1 atm ethylene.
[b] Using toluene (entry 1–12) and pentane (13–29) as internal standard.

higher catalytic activity than the corresponding complexes **12** and **13**. These results agreed well with computational conclusion on the relationship of catalytic activity and net charge of late-transition metal complexes [37]. As to **17**–**24**, the introduction of nitro-group into the ligands impaired the catalytic activity of the corresponding complexes. The orders of the activity are **18** > **17** > **19**, **21** > **22**, **23** > **24** and **18** > **21**.

The oligomerization products of **12**–**24** are mainly C4 and C6. In **14**/MAO system, C_4 is distributed in 40% of 2-methylpropene and 60% of trans-2-butene, while C_6 in 6% of 3-methylpentene, 8% of 1-hexene and 86% of internal olefins (50% of 3-hexene, 10% of 2-hexene and 26% of 3-methyl-2-pentene). The β-hydrogen elimination and chain transformation perhaps play a major role for the distribution of oligomers.

The dependence of catalytic activity on reaction time was studied using **14** and **18**/MAO systems (Table 5). The catalytic activity of **14** decreased from 3.1×10^4 g mol^{-1} h^{-1} in 10 min to 1.2×10^4 g mol^{-1} h^{-1} in 120 min, and remained active in following hours with a little decrease. As to **18**, its activity decreased from 15.2×10^5 g mol^{-1} atm^{-1} h^{-1} in 5 min to 2.11×10^5 g mol^{-1} atm^{-1} h^{-1} in 120 min, however, its activity was completely lost in 3 h. The content of C4 decreased regularly from 92% to 80% in the oligomers produced.

Table 5
Dependence of reaction time on catalytic activity

Entry	Complex[a]	Time (min)	Activity (10^4 g mol^{-1} h^{-1})	Distribution of oligomers (%)[b]	
				C_4	C_6
1	**14**	10	3.1	88	12
2	**14**	30	2.3	87	13
3	**14**	60	1.9	87	13
4	**14**	90	1.3	85	15
5	**14**	120	1.2	87	13
6	**18**	5	152	92	8
7	**18**	15	94.8	86	14
8[c]	**18**	30	49.4	88	12
9	**18**	60	31.3	81	19
10	**18**	90	20.9	82	18
11	**18**	120	21.1	80	20

[a] Reaction condition: entry (1–5) 5 μmol catalyst, 40 ml toluene, Al/Ni 500, 1 h, 25 °C, 1 atm ethylene; entry (6–11) 5 μmol catalyst, 30 ml toluene, Al/Ni 1000, 1 h, 30 °C, 1 atm ethylene.
[b] Using toluene (entry 1–5) and pentane (entry 6–11) as internal standard.
[c] Reaction temperature, 22 °C.

2.4.2. Effect of the addition of PPh_3

The effect of PPh_3 on the ethylene oligomerization was investigated using **14**/MAO system and compared with (DME)$NiBr_2$ (Table 6). The catalytic activity of **14** was much improved from 3.3×10^4 to 1.94×10^5 g mol^{-1} h^{-1} when PPh_3 was added. At the same time, a small amount of octenes (ca. 3%) appeared. In comparison, the catalytic activity of (DME)$NiBr_2$ is very low with values of $0.8–5.4 \times 10^4$ g mol^{-1} h^{-1}.

In order to elucidate the function of PPh_3, ^{31}P NMR spectra of the reaction system of **14** were examined. When one equivalent of PPh_3 was added into the toluene solution of the complex, the color of the solution turned from pale yellow to yellow. The ^{31}P NMR spectrum showed two peaks at −3.95 and 21.36 ppm, which were attributed to the resonance of free and coordinated PPh_3, respectively. The injection of MAO into the reactor made the color of the solution turned to bright brown. In ^{31}P NMR spectrum, the peak of free PPh_3 disappeared and a new peak at 37.69 ppm appeared while the peak at 21.36 ppm shifted slightly to 20.93 ppm. The uptake of ethylene took place slowly at the beginning and accelerated after several minutes.

The existence of the auxiliary PR_3 ligand for the SHOP-type catalysts mainly resulted in the stabilization of the catalytic species [38] and a further report claimed its influence on the ethylene oligomerization [12f]. So we guess that a new kind of catalytic active species is formed during the catalytic process of **14**/MAO system. At the beginning of the reaction, some portion of PPh_3 coordinates to the nickel atom. The addition of MAO depletes the weak acidic amide hydrogen of the ligand and the catalytic active species is formed by the delocalization of the electron on the amide nitrogen to the chelate ring and the coordination of PPh_3 on nickel atom. In fact, the new species is a kind of neutral nickel complex [39].

This proposal was confirmed by the syntheses of the neutral complexes **17**–**24**. It is noticeable that the catalytic activity of the neutral nickel complexes is commonly one order of amount higher than the values of the dinickel complexes. The effect of PPh_3 was also tested using **18**/MAO system. With the increase of the P/Ni molar ratio from 1 to 20, the catalytic activity of **18** continuously decreased from 4.82×10^5 to 1.39×10^5 g mol^{-1} atm^{-1} h^{-1}. At the same time, the content of C_4 increased from 76% to 95%.

3. Experimental

3.1. General procedures

All manipulations for moisture-sensitive compounds were carried out under an atmosphere of nitrogen using standard Schlenk techniques. Melting points (MP) were determined with a digital electrothermal apparatus without calibration. The IR spectra were recorded on a Perkin–Elmer FT-IR 2000 spectrophotometer using KBr disc in the range of 4000–400 cm^{-1} and on a Nicolet Magna-IR 750 in the range of 650–50 cm^{-1}. The ^1H NMR spectra were recorded on a Bruker DMX-300 instrument with TMS as the internal standard. The ^{31}P NMR spectra were recorded on a Varian XL-200 instrument with H_3PO_4 (85%) as the external standard. Splitting patterns are designated as follows: s, singlet; bs, broad singlet; d, doublet; dd, double doublet; t, triplet; m, multiplet. The elemental analyses were performed on a Flash EA 1112 microanalyzer. The ESI-MS was recorded on a Shimadzu LCMS-2010 spectrometer. The

Table 6
Effects of the addition of Ph_3P on ethylene oligomerization

Entry	Complex	PPh_3/Ni (mol/mol)	Activity (10^4 g mol^{-1} h^{-1})	Distribution of oligomers (%)[e]		
				C_4	C_6	C_8
1	**14**[a]	0	3.3	84	16	
2	**14**[b]	0.5	12.8	84	13	3
3	**14**[b]	1	19.4	74	23	3
4	**14**[b]	5	10.1	94	4	2
5	**14**[b]	10	6.6	93	6	1
6	**(DME)$NiBr_2$**[c]	0	0.8	89	11	
7	**(DME)$NiBr_2$**[c]	1	5.4	91	9	
8	**18**[d]	1	48.2	76	24	
9	**18**[d]	2	43.6	78	22	
10	**18**[d]	5	36.3	86	14	
11	**18**[d]	10	17.1	92	8	
12	**18**[d]	20	13.9	95	5	

[a] Reaction condition: 5 μmol catalyst, 40 ml toluene, Al/Ni 500, 1 h, 18 °C, 1 atm ethylene.
[b] Reaction condition: 5 μmol catalyst, 40 ml toluene, Al/Ni 500, 1 h, 25 °C, 1 atm ethylene.
[c] Reaction condition: 10 μmol catalyst, 30 ml toluene, Al/Ni 1000, 1 h, 25 °C, 1 atm ethylene.
[d] Reaction condition: 5 μmol catalyst, 30 ml toluene, Al/Ni 1000, 0.5 h, 30 °C, 1 atm ethylene.
[e] Using toluene (entry 1–7) and pentane (entry 8–12) as internal standard.

MALDI-TOF MS was recorded on a Bruker BIFLEX III spectrometer. Distribution of oligomers obtained was measured on a Varian VISTA 6000 GC spectrometer and a HP 5971A GC-MS detector.

THF and toluene were refluxed over sodium-benzophenone until purple color appeared and distilled under nitrogen atmosphere prior to use. CH_2Cl_2 and pentane were distilled under nitrogen from CaH_2. Pyridine was dried over solid KOH and kept with 4 Å molecule sieves. NaH was washed with pentane (3×20 ml) and dried before use. *trans*-[NiCl(Naph)(PPh_3)$_2$] [40] and *trans*-[NiCl(Ph)(PPh_3)$_2$] [41] were prepared according to literature procedure. (DME)$NiBr_2$ and 2-aminopyridines were purchased from Alfa Aesar and Aldrich Chem. Co., respectively. Methylaluminoxane (MAO, 1.4 mol l^{-1} in toluene) was purchased from Albemarle Corp. (USA). All other chemicals were obtained commercially and used without further purification unless stated otherwise.

3.2. Synthesis of N-(2-pyridyl)benzamides

3.2.1. N-(6-Methyl-2-pyridyl)benzamide (**1**)

Benzoic chloride (1.41 g, 1.2 ml, 10 mmol) in 10 ml of THF was added dropwise to the solution of 2-amino-6-methylpyridine (1.08 g, 10 mmol) in 10 ml of dry pyridine at 20 °C. The reaction mixture was stirred for 12 h at room temperature and quenched in water (400 ml) to afford a white solid in 99% yield (2.05 g). MP: 78–80 °C. FT-IR (KBr disc, cm^{-1}): 3192 (m), 1677 (s), 1577 (s), 1459 (s), 1304 (s), 1129 (m), 790 (m), 719 (m). ^{1}H NMR (300 MHz, $CDCl_3$/ppm): 2.47 (s, 3H, CH_3), 6.94 (d, 1H, $J = 7.43$ Hz), 7.53 (m, 3H), 7.66 (t, 1H, $J = 7.85$ Hz), 7.94 (d, 2H, $J = 7.61$ Hz), 8.20 (d, 1H, $J = 8.29$ Hz), 8.62 (bs, 1H, NH). *Anal.* Calc. for $C_{13}H_{12}N_2O$ (212.25): C, 73.56; H, 5.70; N, 13.20. Found: C, 73.77; H, 5.73; N, 12.98%.

3.2.2. N-(4,6-Dimethyl-2-pyridyl)benzamide (**2**)

In a similar manner as described for **1**, the compound **2** was prepared from 2-amino-4,6-dimethylpyridine and benzoic chloride as white solid in 63% yield (1.43 g). MP: 128–130 °C. FT-IR (KBr disc, cm^{-1}): 3183 (w), 1676 (s), 1614 (m), 1567 (s), 1421 (s), 1282 (s), 846 (w), 706 (s). ^{1}H NMR (300 MHz, $CDCl_3$/ppm): 2.37 (s, 3H, CH_3), 2.43 (s, 3H, CH_3), 6.78 (s, 1H), 7.52 (m, 3H), 7.93 (d, 2H, $J = 7.31$ Hz), 8.05 (s, 1H), 8.45 (bs, 1H, NH). *Anal.* Calc. for $C_{14}H_{14}N_2O$ (226.27): C, 74.31; H, 6.24; N, 12.38. Found: C, 74.43; H, 6.24; N, 12.17%.

3.2.3. N-(6-Ethyl-2-pyridyl)benzamide (**3**)

In a similar manner as described for **1**, the compound **3** was prepared from 2-amino-6-ethylpyridine and benzoic chloride as white solid in 78% yield (1.76 g). MP: 80–82 °C. FT-IR (KBr disc, cm^{-1}): 3280 (m), 1652 (s), 1601 (m), 1538 (m), 1449 (s), 1308 (s), 812 (s), 714 (s). ^{1}H NMR (300 MHz, $CDCl_3$/ppm): 1.34 (t, 3H, $J = 7.61$ Hz, CH_3), 2.78 (dd, 2H, $J = 7.60$ Hz, CH_2), 6.99 (d, 1H, $J = 7.50$ Hz), 7.58 (m, 3H), 7.72 (t, 1H, $J = 7.87$ Hz), 7.99 (d, 2H, $J = 7.36$ Hz), 8.24 (d, 1H, $J = 8.23$ Hz), 8.65 (bs, 1H, NH). *Anal.* Calc. for $C_{14}H_{14}N_2O$ (226.27): C, 74.31; H, 6.24; N, 12.38. Found: C, 74.32; H, 6.22; N, 12.34%.

3.2.4. N-(6-Methyl-2-pyridyl)-4-nitrobenzamide (**4**)

In a similar manner as described for **1**, the compound **4** was prepared from 2-amino-6-methylpyridine and 4-nitrobenzoic chloride as white solid in 97% yield (2.50 g). MP: 130–131 °C. FT-IR (KBr disc, cm^{-1}): 3343 (m), 1653 (s), 1602 (s), 1528 (s), 1453 (s), 1349 (m), 854 (m), 791 (m), 716 (m). ^{1}H NMR (300 MHz, $CDCl_3$/ppm): 2.49 (s, 3H, CH_3), 6.99 (d, 1H, $J = 7.49$ Hz), 7.69 (t, 1H, $J = 7.91$ Hz), 8.10 (d, 2H, $J = 8.59$ Hz), 8.16 (d, 1H, $J = 8.24$ Hz), 8.36 (d, 2H, $J = 8.78$ Hz), 8.58 (bs, 1H, NH). *Anal.* Calc. for $C_{13}H_{11}N_3O_3$ (257.24): C, 60.70; H, 4.31; N, 16.33. Found: C, 60.02; H, 4.24; N, 15.95%.

3.2.5. N-(4,6-Dimethyl-2-pyridyl)-4-nitrobenzamide (**5**)

In a similar manner as described for **1**, the compound **5** was prepared from 2-amino-4,6-dimethylpyridine and 4-nitrobenzoic chloride as white solid in 83% yield (2.24 g). MP: 156–158 °C. FT-IR (KBr disc, cm^{-1}): 3326 (w), 1655 (s), 1606 (w), 1526 (s), 1439 (s), 1345 (s), 1285 (w), 849 (m), 716 (m). ^{1}H NMR (300 MHz, $CDCl_3$/ppm): 2.38 (s, 3H, CH_3), 2.43 (s, 3H, CH_3), 6.83 (s, 1H), 8.01 (s, 1H), 8.09 (d, 2H, $J = 8.75$ Hz), 8.35 (d, 2H, $J = 8.65$ Hz), 8.57 (bs, 1H, NH). *Anal.* Calc. for $C_{14}H_{13}N_3O_3$ (271.27): C, 61.99; H, 4.83; N, 15.49. Found: C, 61.59; H, 4.80; N, 15.49%.

3.2.6. N-(2-Pyridyl)benzamide (**6**)

In a similar manner as described for **1**, the compound **6** was prepared from 2-aminopyridine and benzoic chloride as white solid in 63% yield (1.24g). MP: 68–70 °C. FT-IR (KBr disc, cm^{-1}): 3170 (br), 1674 (s), 1580 (s), 1531 (s), 1435 (s), 1305 (s), 777 (m), 722 (m). ^{1}H NMR (300 MHz, $CDCl_3$/ppm): 7.09 (t, 1H, $J = 6.10$ Hz), 7.45 –7.62 (m, 3H), 7.78 (t, 1H, $J = 7.47$ Hz), 7.95 (d, 2H, $J = 7.48$ Hz), 8.30 (d, 1H, $J = 4.72$ Hz), 8.42 (d, 1H, $J = 8.33$ Hz), 8.69 (bs, 1H, NH). *Anal.* Calc. for $C_{12}H_{10}N_2O$ (198.22): C, 72.71; H, 5.08; N, 14.13. Found: C, 72.88; H, 5.05; N, 13.83%.

3.2.7. N-(4-Methyl-2-pyridyl)benzamide (**7**)

In a similar manner as described for **1**, the compound **7** was prepared from 2-amino-4-methylpyridine and benzoic chloride as white solid in 50% yield (1.07 g). MP: 106–108 °C. FT-IR (KBr disc, cm^{-1}): 3308 (s), 1661 (s), 1535 (s), 1411 (s), 1301 (s), 1164 (m), 705 (s). ^{1}H NMR (300 MHz, $CDCl_3$/ppm): 2.44 (s, 3H, CH_3), 6.93

(d, 1H, $J = 5.03$ Hz), 7.50–7.63 (m, 3H), 7.96 (d, 2H, $J = 7.28$ Hz), 8.14 (d, 1H, $J = 5.10$ Hz), 8.28 (s, 1H), 8.74 (bs, 1H, NH). *Anal*. Calc. for $C_{13}H_{12}N_2O$ (212.25): C, 73.56; H, 5.70; N, 13.20. Found: C, 73.74; H, 5.73; N, 12.84%.

3.2.8. N-(5-Nitro-2-pyridyl)benzamide (8)

In a similar manner as described for **1**, the compound **8** was prepared from 2-amino-5-nitropyridine and benzoic chloride as white solid in 96% yield (2.15g). MP: 165–167 °C. FT-IR (KBr disc, cm^{-1}): 3347 (m), 1689 (s), 1601 (s), 1514 (s), 1395 (m), 1343 (s), 1234 (s), 1120 (s), 852 (m), 716 (m). ^1H NMR (300 MHz, $CDCl_3$/ppm): 7.55 (t, 2H, $J = 7.49$ Hz), 7.64 (t, 1H, $J = 7.21$ Hz), 7.95 (d, 2H, $J = 7.61$ Hz), 8.58 (m, 2H), 8.94 (bs, 1H, NH), 9.16 (s, 1H). *Anal*. Calc. for $C_{12}H_9N_3O_3$ (243.22): C, 59.26; H, 3.73; N, 17.28. Found: C, 59.22; H, 3.72; N, 16.91%.

3.2.9. N-(2-Pyridyl)-4-nitrobenzamide (9)

In a similar manner as described for **1**, the compound **9** was prepared from 2-aminopyridine and 4-nitrobenzoic chloride as white solid in 55% yield (1.25g). MP: 236–238 °C. FT-IR (KBr disc, cm^{-1}): 3347 (m), 1679 (s), 1584 (s), 1515 (s), 1438 (m), 1312 (s), 853 (m), 790 (m), 716 (m). ^1H NMR (300 MHz, $CDCl_3$/ppm): 7.11 (t, 1H, $J = 6.10$ Hz), 7.78 (t, 1H, $J = 7.89$ Hz), 8.07 (d, 2H, $J = 8.46$ Hz), 8.33 (t, 4H, $J = 7.71$ Hz), 8.58 (bs, 1H, NH). *Anal*. Calc. for $C_{12}H_9N_3O_3$ (243.22): C, 59.26; H, 3.73; N, 17.28. Found: C, 59.23; H, 3.73; N, 17.23%.

3.2.10. N-(4-Methyl-2-pyridyl)-4-nitrobenzamide (10)

In a similar manner as described for **1**, the compound **10** was prepared from 2-amino-4-methylpyridine and 4-nitrobenzoic chloride as white solid in 90% yield (2.30 g). MP: 182–184 °C. FT-IR (KBr disc, cm^{-1}): 3347 (m), 1659 (s), 1606 (m), 1533 (s), 1349 (m), 1300 (m), 854 (m), 717 (m). ^1H NMR (300 MHz, $CDCl_3$/ppm): 2.43 (s, 3H, CH_3), 6.95 (d, 1H, $J = 4.95$ Hz), 7.88–8.25 (m, 4H), 8.35 (d, 2H, $J = 8.63$ Hz), 8.81 (bs, 1H, NH). *Anal*. Calc. for $C_{13}H_{11}N_3O_3$ (257.24): C, 60.70; H, 4.31; N, 16.33. Found: C, 59.90; H, 4.17; N, 15.81%.

3.2.11. N-(5-Nitro-2-pyridyl)-4-nitrobenzamide (11)

In a similar manner as described for **1**, the compound **11** was prepared from 2-amino-5-nitropyridine and 4-nitrobenzoic chloride as white solid in 87% yield (2.46 g). MP: 216–218 °C. FT-IR (KBr disc, cm^{-1}): 3394 (m), 1691 (s), 1606 (s), 1513 (s), 1350 (s), 1299 (s), 1225 (m), 1118 (m), 850 (m), 714 (m). ^1H NMR (300 MHz, $CDCl_3$/ppm): 6.94 (d, 1H, $J = 4.78$ Hz), 7.87 –8.24 (m, 4H), 8.35 (d, 2H, $J = 8.46$ Hz), 8.72 (bs, 1H, NH). *Anal*. Calc. for $C_{12}H_8N_4O_5$ (288.22): C, 50.01; H, 2.80; N, 19.44. Found: C, 49.82; H, 2.57; N, 19.67%.

3.3. Synthesis of complexes

3.3.1. [N-(6-Methyl-2-pyridyl)benzamide]dinickel(II) di-μ-bromide dibromide (12)

A solution of the ligand **1** (240 mg, 1.1 mmol) in THF (10 ml) was added to the solution of (DME)$NiBr_2$ (308 mg, 1 mmol) in THF (60 ml). The mixture was stirred at room temperature for 12 h. The resulting precipitate was filtered, washed with 5 ml of THF and dried in vacuo to result a yellow powder in 83% yield (357 mg). MP: 290 °C (dec.). FT-IR (KBr disc, cm^{-1}): 3273 (br), 1626 (s), 1577 (w), 1533 (s), 1461 (m), 1417 (w), 1315 (m), 1228 (w), 797 (m), 706 (s), 237 (s), 111 (m). *Anal*. Calc. for $C_{26}H_{24}Br_4N_4Ni_2O_2$ (861.50): C, 36.25; H, 2.81; N, 6.50. Found: C, 36.99; H, 2.87; N, 6.59%.

3.3.2. [N-(4,6-Dimethyl-2-pyridyl)benzamide]dinickel(II) di-μ-bromide dibromide (13)

In a similar manner described for **12**, the compound **13** was obtained from (DME)$NiBr_2$ and ligand **2** as an orange-red powder in 68% yield (303 mg). MP: 300 °C (dec.). FT-IR (KBr disc, cm^{-1}): 3243 (br), 1629 (s), 1575 (s), 1530 (s), 1459 (s), 1310 (m), 847 (m), 706 (s), 231 (s), 95 (m). *Anal*. Calc. for $C_{28}H_{28}Br_4N_4Ni_2O_2$ (889.55): C, 37.81; H, 3.17; N, 6.30. Found: C, 37.57; H, 3.16; N, 6.18%.

3.3.3. [N-(6-Ethyl-2-pyridyl)benzamide]dinickel(II) di-μ-bromide dibromide (14)

In a similar manner described for **12**, the compound **14** was obtained from (DME)$NiBr_2$ and **3** as a yellow powder in 72% yield (322 mg). MP:>320 °C. FT-IR (KBr disc, cm^{-1}): 3369 (br), 1624 (s), 1578 (w), 1534 (m), 1456 (s), 810 (w), 700 (m), 185 (s), 105 (m). *Anal*. Calc. for $C_{28}H_{28}Br_4N_4Ni_2O_2$ (889.55): C, 37.81; H, 3.17; N, 6.30. Found: C, 37.77; H, 3.23; N, 6.01%.

3.3.4. [N-(6-Methyl-2-pyridyl)-4-nitrobenzamide]dinickel(II) di-μ-bromide dibromide (15)

In a similar manner described for **12**, the compound **15** was obtained from (DME)$NiBr_2$ and **4** as a yellow powder in 50% yield (237 mg). MP: 305 °C (dec.). FT-IR (KBr disc, cm^{-1}): 3372 (br), 1630 (s), 1604 (m), 1534 (s), 1461 (s), 1348 (s), 850 (m), 712 (m), 216 (s), 118 (m). *Anal*. Calc. for $C_{26}H_{22}Br_4N_6Ni_2O_6$ (951.49): C, 32.82; H, 2.33; N, 8.83. Found: C, 32.65; H, 2.39; N, 8.64%.

3.3.5. [N-(4,6-Dimethyl-2-pyridyl)-4-nitrobenzamide]dinickel(II) di-μ-bromide dibromide (16)

In a similar manner described for **12**, the compound **16** was obtained from (DME)$NiBr_2$ and **5** as a yellow powder in 68% yield (331 mg). MP: 290 °C (dec.). FT-IR (KBr disc, cm^{-1}): 3386 (br), 1636 (s), 1530 (s), 1446 (m), 1345 (s), 851 (m), 711 (m), 228 (s), 123 (m). *Anal*. Calc. for $C_{28}H_{26}Br_4N_6Ni_2O_6$ (979.55): C, 34.33; H, 2.68; N, 8.58. Found: C, 34.31; H, 2.78; N, 8.40%.

*3.3.6. (1-Naphthyl)[N-(2-pyridyl)benzamido](triphenylphosphine)nickel(II) (**17**)*

A flame-dried Schlenk tube was charged with **6** (198 mg, 1 mmol) and sodium hydride (64 mg, 2.7 mmol) under nitrogen. THF (10 ml) was added to the mixture at 0 °C. Many bubbles were immediately produced. The resulting mixture was stirred at room temperature for 1 h, filtered, and evaporated. The solid was washed with pentane and dried in vacuo. The Na salt was immediately used in the next step without further purification. Solid *trans*-[NiCl(Naph)(PPh_3)$_2$] (746 mg, 1 mmol) was added to the Schlenk tube under positive nitrogen flow. The mixture was charged with toluene (30 ml) and stirred at 20 °C for 16 h. Then, the reaction mixture was filtered and the filtrate was concentrated in vacuo to ca. 5 ml. Hexane (50 ml) was added to this solution. A solid was precipitated and isolated by cannula filtration to get a yellow-brown powder in 79% yield (509 mg). MP: 200–202 °C. FT-IR (KBr disc, cm^{-1}): 3429 (br), 3051 (w), 1559 (m), 1504 (m), 1436 (s), 1393 (m), 781(m), 696 (m). ^1H NMR (300 MHz, $CDCl_3$/ppm): 6.19 (t, 1H, $J = 6.54$ Hz), 6.81 (t, 1H, $J = 7.43$ Hz), 6.91 (d, 1H, $J = 6.60$ Hz), 7.00 (t, 2H, $J = 7.61$ Hz), 7.08–7.97 (m, 25H), 9.58 (d, 1H, $J = 8.06$ Hz). ^{31}P NMR (H_3PO_4 as external standard, toluene/ppm): 28.25. *Anal.* Calc. for $C_{40}H_{31}N_2NiOP$ (645.35): C, 74.44; H, 4.84; N, 4.34. Found: C, 74.98; H, 5.22; N, 4.20%.

*3.3.7. (1-Naphthyl)[N-(4-methyl-2-pyridyl)benzamido](triphenylphosphine)nickel(II) (**18**)*

In a similar manner described for **17**, the compound **18** was obtained from *trans*-[NiCl(Naph)(PPh_3)$_2$] and **7** as a yellow powder in 65% yield (430 mg). MP: 134–136 °C. FT-IR (KBr disc, cm^{-1}): 3432 (br), 3052 (w), 1556 (m), 1500 (m), 1441 (s), 1379 (m), 697 (m). ^1H NMR (300 MHz, $CDCl_3$/ppm): 2.14 (s, 3H, CH_3), 6.03 (d, 1H, $J = 6.40$ Hz), 6.74 (d, 1H, $J = 6.55$Hz), 6.78 (t, 1H, $J = 7.45$ Hz), 6.97 (t, 3H, $J = 7.55$ Hz), 7.06–7.56 (m, 23H), 9.55 (d, 1H, $J = 8.04$ Hz). ^{31}P NMR (H_3PO_4 as external standard, toluene/ppm): 28.82. *Anal.* Calc. for $C_{41}H_{33}N_2NiOP$ (659.38): C, 74.68; H, 5.04; N, 4.25. Found: C, 75.13; H, 5.14; N, 4.03%. Positive MALDI-TOF MS: ion at *m/e* 659.4 {$[C_{41}H_{33}N_2NiOP]^+$, 100%}.

*3.3.8. (1-Naphthyl)[N-(5-nitro-2-pyridyl)benzamido](triphenylphosphine)nickel(II) (**19**)*

In a similar manner described for **17**, the compound **19** was obtained from *trans*-[NiCl(Naph)(PPh_3)$_2$] and **8** as a red powder in 62% yield (520 mg). MP: 156–158 °C. FT-IR (KBr disc, cm^{-1}): 3053 (w), 1570 (m), 1490 (m), 1459 (m), 1433 (s), 1331 (s), 696 (m). ^1H NMR (300 MHz, $CDCl_3$/ppm): 6.64 (t, 1H, $J = 7.41$ Hz), 6.79–7.70 (m, 27H), 8.03 (d, 1H, $J = 8.80$ Hz), 9.35 (d, 1H, $J = 7.64$ Hz). ^{31}P NMR (H_3PO_4 as external standard, toluene/ppm): 28.20. *Anal.* Calc. for $C_{40}H_{30}N_3NiO_3P \cdot C_7H_8$ (782.49): C, 72.14; H, 4.89; N, 5.37. Found: C, 71.81; H, 4.93; N, 5.40%.

*3.3.9. (1-Naphthyl)[N-(2-Pyridyl)-4-nitrobenzamido](triphenylphosphine)nickel(II) (**20**)*

In a similar manner described for **17**, the compound **20** was obtained from *trans*-[NiCl(Naph)(PPh_3)$_2$] and **9** as a yellow powder in 68% yield (463 mg). MP: 200–202 °C. FT-IR (KBr disc, cm^{-1}): 3051 (w), 1566 (s), 1523 (s), 1457 (s), 1432 (s), 1344 (s), 696 (m). ^1H NMR (300 MHz, $CDCl_3$/ppm): 6.25 (t, 1H, $J = 6.51$ Hz), 6.81 (t, 1H, $J = 7.37$ Hz), 6.92 (d, 1H, $J = 7.37$ Hz), 7.09–7.57 (m, 24H), 7.82 (d, 2H, $J = 8.62$ Hz), 9.53 (d, 1H, $J = 8.62$ Hz). ^{31}P NMR (H_3PO_4 as external standard, toluene/ppm): 28.57. *Anal.* Calc. for $C_{40}H_{30}N_3NiO_3P$ (690.35): C, 69.59; H, 4.38; N, 6.09. Found: C, 69.80; H, 4.40; N, 6.23%.

*3.3.10. (1-Naphthyl)[N-(4-methyl-2-pyridyl)-4-nitrobenzamido](triphenylphosphine)nickel(II) (**21**)*

In a similar manner described for **17**, the compound **21** was obtained from *trans*-[NiCl(Naph)(PPh_3)$_2$] and **10** as a yellow powder in 68% yield (475 mg). MP: >196 °C (dec.). FT-IR (KBr disc, cm^{-1}): 3429 (br), 3051 (w), 1577 (m), 1522 (m), 1455 (s), 1330 (s), 1105 (m), 695 (m). ^1H NMR (300 MHz, $CDCl_3$/ppm): 2.17 (s, 3H, CH_3), 6.11 (d, 1H, $J = 6.09$ Hz), 6.79–7.53 (m, 25H), 7.83 (d, 2H, $J = 8.71$ Hz), 9.54 (d, 1H, $J = 8.05$ Hz). ^{31}P NMR (H_3PO_4 as external standard, toluene/ppm): 28.69. *Anal.* Calc. for $C_{41}H_{32}N_3NiO_3P$ (704.38): C, 69.91; H, 4.58; N, 5.97. Found: C, 69.19; H, 4.53; N, 5.97%.

*3.3.11. (1-Naphthyl)[N-(5-nitro-2-pyridyl)-4-nitrobenzamido](triphenylphosphine)nickel(II) (**22**)*

In a similar manner described for **17**, the compound **22** was obtained from *trans*-[NiCl(Naph)(PPh_3)$_2$] and **11** as a red powder in 53% yield (422 mg). MP: 230–232 °C. FT-IR (KBr disc, cm^{-1}): 3429 (br), 3051 (w), 1577 (m), 1522 (m), 1455 (s), 1330 (s), 1130 (s), 1105 (m), 695 (m). ^1H NMR (300 MHz, $CDCl_3$/ppm): 6.92 (t, 1H, $J = 7.39$ Hz), 7.15–7.74 (m, 24H), 7.87 (d, 2H, $J = 8.33$), 8.18 (d, 1H, $J = 9.05$ Hz), 9.40 (d, 1H, $J = 7.69$ Hz). ^{31}P NMR (H_3PO_4 as external standard, toluene/ppm): 28.42. *Anal.* Calc. for $C_{40}H_{29}N_4NiO_5P$ (735.35): C, 65.33; H, 3.98; N, 7.62. Found: C, 64.98; H, 3.85; N, 7.76%.

*3.3.12. [N-(5-Nitro-2-pyridyl)benzamido](phenyl)(triphenylphosphine)nickel(II) (**23**)*

In a similar manner described for **17**, the compound **23** was obtained from *trans*-[NiCl(Ph)(PPh_3)$_2$] and **8** as a red powder in 58% yield (371 mg). MP: 174 °C (dec.). FT-IR (KBr disc, cm^{-1}): 3445 (br), 3053 (w), 1568 (m), 1492 (m), 1433 (s), 1328 (s), 1107 (m), 698 (m). ^1H NMR (300 MHz, $CDCl_3$/ppm): 6.71 (m, 3H), 7.04–7.60 (m, 24H), 7.99 (s, 1H), 8.19 (dd, 1H, $J = 9.15$ Hz). ^{31}P NMR (H_3PO_4 as external standard, toluene / ppm):

Table 7
Crystal data and structure refinement for **12**, **14**, **17**, **19** and **23**

Complex	**12**	**14**	**17**	**19**	**23**
Formula	$C_{26}H_{24}Br_4N_4Ni_2O_2$	$C_{28}H_{28}Br_4N_4Ni_2O_2$	$C_{40}H_{31}N_2NiOP$	$C_{40}H_{30}N_3NiO_3P \cdot C_4H_8O$	$C_{36}H_{28}N_3NiO_3P$
Formula weight	861.56	889.55	649.35	762.45	640.29
Temperature (K)	293(2)	293(2)	293(2)	293(2)	293(2)
Wavelength (Å)	0.71073	0.71073	0.71073	0.71073	0.71073
Crystal system	triclinic	triclinic	triclinic	triclinic	triclinic
Space group	$P\bar{1}$	$P\bar{1}$	$P\bar{1}$	$P\bar{1}$	$P\bar{1}$
a (Å)	8.683(2)	8.644(2)	10.650(2)	11.420(2)	10.672(3)
b (Å)	9.413(2)	9.523(2)	11.314(2)	12.927(3)	12.192(4)
c (Å)	10.622(2)	10.637(2)	14.858(3)	14.748(3)	12.658(4)
α (°)	112.31(3)	69.10(3)	93.07(3)	75.44(3)	100.802(5)
β (°)	93.64(3)	74.00(3)	109.00(3)	78.87(3)	90.173(4)
γ (°)	113.64(3)	72.82(3)	103.49(3)	73.66(3)	106.390(4)
Volume (Å^3)	711.6(2)	767.1(3)	1629.6(6)	2004.5(7)	1549.3(8)
Z	1	1	2	2	2
D_{calc} (Mg m^{-3})	2.011	1.926	1.334	1.263	1.373
μ (mm^{-1})	6.970	6.469	0.680	0.569	0.719
Crystal size (mm^3)	$0.223 \times 0.218 \times 0.122$	$0.307 \times 0.205 \times 0.118$	$0.528 \times 0.407 \times 0.266$	$0.355 \times 0.200 \times 0.141$	$0.24 \times 0.22 \times 0.20$
θ Range (°)	2.63–27.45	2.09–27.48	2.53–27.49	1.68–27.48	1.99–26.39
Limiting indices	$-10 \leqslant h \leqslant 11$, $-12 \leqslant k \leqslant 12$, $-13 \leqslant l \leqslant 13$	$0 \leqslant h \leqslant 11$, $-11 \leqslant k \leqslant 12$, $-12 \leqslant l \leqslant 13$	$0 \leqslant h \leqslant 13$, $-14 \leqslant k \leqslant 14$, $-19 \leqslant l \leqslant 18$	$-14 \leqslant h \leqslant 14$, $-15 \leqslant k \leqslant 16$, $-18 \leqslant l \leqslant 19$	$-13 \leqslant h \leqslant 12$, $-8 \leqslant k \leqslant 15$, $-15 \leqslant l \leqslant 15$
Reflections collected	4765	5968	6388	11546	8991
Unique reflections	3149 [$R_{int} = 0.0436$]	3229 [$R_{int} = 0.0884$]	6388 [$R_{int} = 0.0405$]	8209 [$R_{int} = 0.1635$]	6275[$R_{int} = 0.0181$]
Completeness to θ (%)	96.6 ($\theta = 27.45°$)	92.1 ($\theta = 27.48°$)	85.4 ($\theta = 27.49°$)	89.4 ($\theta = 27.48°$)	99.6 ($\theta = 25.00°$)
Absorption correction	ABSCOR	ABSCOR	ABSCOR	ABSCOR	SADABS
Maximum/minimum transmission	1.2650/0.7147	1.5527/0.3311	1.3088/0.6989	1.4561/0.5982	1.0000/0.8783
Data/restraints/parameters	3149/0/177	3229/0/185	6388/0/406	8209/9/478	6275/0/397
Goodness-of-fit on F^2	0.790	0.813	0.713	0.646	1.013
R indices [$I > 2\sigma(I)$]	$R_1 = 0.0392$, $wR_2 = 0.0679$	$R_1 = 0.0652$, $wR_2 = 0.1351$	$R_1 = 0.0479$, $wR_2 = 0.0900$	$R_1 = 0.0685$, $wR_2 = 0.1177$	$R_1 = 0.0379$, $wR_2 = 0.0828$
R indices (all data)	$R_1 = 0.0805$, $wR_2 = 0.0736$	$R_1 = 0.1313$, $wR_2 = 0.1511$	$R_1 = 0.1969$, $wR_2 = 0.1131$	$R_1 = 0.3519$, $wR_2 = 0.1625$	$R_1 = 0.0634$, $wR_2 = 0.0941$
Largest difference peak and hole (e A^{-3})	0.676 and −0.532	1.200 and −0.863	0.311 and −0.175	0.324 and −0.237	0.275 and −0.249

29.22. *Anal.* Calc. for $C_{36}H_{28}N_3NiO_3P$ (640.29): C, 67.53; H, 4.41; N, 6.56. Found: C, 67.82; H, 4.48; N, 6.76%.

3.3.13. [N-(5-Nitro-2-pyridyl)-4-nitrobenzamido](phenyl)(triphenylphosphine)nickel(II) (**24**)

In a similar manner described for **17**, the compound **24** was obtained from *trans*-[NiCl(Ph)(PPh_3)$_2$] and **11** as a red powder in 61% yield (418 mg). MP: 180 °C (dec.). FT-IR (KBr disc, cm^{-1}): 3431 (br), 3053 (w), 1578 (m), 1523 (m), 1456 (s), 1328 (s), 1107 (m), 696 (m). ^1H NMR (300 MHz, $CDCl_3$/ppm): 6.62 (m, 3H), 7.08–7.76 (m, 21H), 7.95 (s, 1H), 8.17 (d, 1H, $J = 7.58$ Hz). ^{31}P NMR (H_3PO_4 as external standard, toluene/ppm): 29.45. *Anal.* Calc. for $C_{36}H_{27}N_4NiO_5P$ (685.29): C, 63.10; H, 3.97; N, 8.18. Found: C, 63.25; H, 3.98; N, 8.07%.

3.4. X-ray crystal structure determination of **12**, **14**, **17**, **19** and **23**

Intensity datasets of **12**, **14**, **17** and **19** were collected at 293 K on a Rigaku RAXIS pid IP diffractometer with graphite-monochromated Mo Kα ($\lambda = 0.71073$ Å) radiation, using the $\omega - 2\theta$ scan mode. Cell parameters were obtained by the global refinement of the positions of all collected reflections. Intensity data were corrected by Lorentz and polarization effects and empirical absorptions were applied by using ABSCOR program. The structure was solved by direct methods. The final refinement was done by full-matrix least-squares on F^2 methods with anisotropic thermal parameters for non-hydrogen atoms and isotropic thermal parameters for geometric hydrogen atoms by using SHELX-97 package [42].

Intensity data of **23** were collected at 293(2) K on a Bruker SMART 1000 CCD diffractometer with graphite-monochromated Mo Kα ($\lambda = 0.71073$ Å) radiation. Data collection and reduction were performed using SMART and SAINT software [43]. Empirical absorption correction was applied to the raw intensities by using SADABS program [44]. The structure was solved by direct methods and full-matrix least-squares method based on F^2 using SHELXTL program package [45]. Non-hydrogen atoms were subjected to anisotropic refinement (see Table 7).

3.5. General procedure for ethylene oligomerization

A flame dried three-neck round flask was loaded with the complex (**12**–**24**) and vacuum-filled three times by nitrogen. Then ethylene was charged together with freshly distilled toluene and stirred for 10 min. MAO was added by a syringe. The reaction mixture was stirred under 1 atm ethylene pressure for a limited time and the catalytic reaction was terminated with acidified water. An aliquot of the reaction mixture was analyzed by GC and GC-MS.

4. Supplementary material

Crystallographic data have been deposited to the Cambridge Crystallographic Data Center, CCDC 212587 for **12**, 212588 for **14**, 223946 for **17**, 223945 for **19** and 223947 for **23**. Copies of the information may be obtained free of charge from the Director, CCDC, 12 Union Road, Cambridge CB2 1EZ, UK (fax: +44-1223-336-033; e-mail: deposit@ccdc.cam.ac.uk or http://www.ccdc.ac.uk), upon request.

Acknowledgements

The authors are grateful to the National Natural Science Foundation of China for the financial support with Grant No. 20272062 and Polymer Chemistry Laboratory, Chinese Academy of Sciences and China Petro-Chemical Corporation for their help.

References

[1] W. Keim, Angew. Chem., Int. Ed. Engl. 29 (1990) 235.
[2] J. Skupińska, Chem. Rev. 91 (1991) 613.
[3] G.J.P. Britovsek, V.C. Gibson, D.F. Wass, Angew. Chem., Int. Ed. Engl. 38 (1999) 429.
[4] S.D. Ittel, L.K. Johnson, M. Brookhart, Chem. Rev. 100 (2000) 1169.
[5] S. Mecking, Angew. Chem., Int. Ed. Engl. 40 (2001) 534.
[6] V.C. Gibson, S.K. Spitzmesser, Chem. Rev. 103 (2003) 283.
[7] L.K. Johnson, C.M. Killian, M. Brookhart, J. Am. Chem. Soc. 117 (1995) 6414.
[8] (a) B.L. Small, M. Brookhart, A.M.A. Bennett, J. Am. Chem. Soc. 120 (1998) 4049;
(b) G.J.P. Britovsek, V.C. Gibson, B.S. Kimberley, P.J. Maddox, S.J. McTavish, G.A. Solan, A.J.P. White, D.J. Williams, Chem. Commun. (1998) 849;
(c) G.J.P. Britovsek, M. Bruce, V.C. Gibson, B.S. Kimberley, P.J. Maddox, S. Mastroianni, S.J. McTavish, C. Redshaw, G.A. Solan, S. Stromberg, A.J.P. White, D.J. Williams, J. Am. Chem. Soc. 121 (1999) 8728.
[9] (a) C.M. Killian, L.K. Johnson, M. Brookhart, Organometallics 16 (1997) 2005;
(b) S.A. Svejda, M. Brookhart, Organometallics 18 (1999) 65.
[10] B.L. Small, M. Brookhart, J. Am. Chem. Soc. 120 (1998) 7143.
[11] G.J.P. Britovsek, S. Mastroianni, G.A. Solan, S.P.D. Baugh, C. Redshaw, V.C. Gibson, A.J.D. White, D.J. Williams, M.R.J. Elsegood, Chem. Eur. J. 6 (2000) 2221.
[12] (a) W. Keim, F.H. Kowaldt, R. Goddard, C. Krüger, Angew. Chem., Int. Ed. Engl. 17 (1978) 466;
(b) M. Peuckert, W. Keim, Organometallics 2 (1983) 594;
(c) W. Keim, A. Behr, B. Gruber, B. Hoffmann, F.H. Kowaldt, U. Kürschner, B. Limbäcker, F.P. Sisting, Organometallics 5 (1986) 2356;
(d) W. Keim, R.P. Schulz, J. Mol. Catal. 92 (1994) 21;
(e) M.C. Bonnet, F. Dahan, A. Ecke, W. Keim, R.P. Schulz, I. Tkatchenko, Chem. Commun. (1994) 615;
(f) J. Pietsch, P. Braunstein, Y. Chauvin, New J. Chem. 22 (1998) 467;
(g) J. Heinicke, M. He, A. Dal, H.F. Klein, O. Hetche, W. Keim, U. Flörke, H.J. Haupt, Eur. J. Inorg. Chem. (2000) 431.

[13] K.A. Ostoja-Starzewski, J. Witte, Angew. Chem., Int. Ed. Engl. 24 (1985) 599;
Angew. Chem., Int. Ed. Engl. 26 (1987) 63.
[14] U. Klabunde, S.D. Ittel, J. Mol. Catal. 41 (1987) 123.
[15] D. Matt, M. Huhn, J. Fischer, A. DeCian, W. Kläui, I. Tkatchenko, M.C. Bonnet, J. Chem. Soc., Dalton Trans. (1993) 1173.
[16] J. Pietsch, P. Braunstein, Y. Chauvin, New J. Chem. 22 (1998) 467.
[17] V.C. Gibson, A. Tomov, A.J.P. White, D.J. Williams, Chem. Commun. (2001) 719.
[18] R. Soula, J.P. Broyer, M.F. Llauro, A. Tomov, R. Spitz, J. Claverie, X. Drujon, J. Malinge, T. Saudemont, Macromolecules 34 (2001) 2438.
[19] (a) Z.J.A. Komon, X. Bu, G.C. Bazan, J. Am. Chem. Soc. 122 (2000) 12379;
(b) B.Y. Lee, X. Bu, G.C. Bazan, Organometallics 20 (2001) 5425;
(c) B.Y. Lee, G.C. Bazan, J. Vela, Z.J.A. Komon, X. Bu, J. Am. Chem. Soc. 123 (2001) 5352;
(d) Y.H. Kim, T.H. Kim, B.Y. Lee, D. Woodmansee, X. Bu, G.C. Bazan, Organometallics 21 (2002) 3082.
[20] (a) S.Y. Desjardins, K.J. Cavell, H. Jin, B.W. Skelton, A.H. White, J. Organomet. Chem. 515 (1996) 233;
(b) S.Y. Desjardins, K.J. Cavell, J.L. Hoare, B.W. Skelton, A.N. Sobolev, A.W. White, W. Keim, J. Organomet. Chem. 544 (1997) 163.
[21] (a) C. Wang, S. Friedrich, T.R. Younkin, R.T. Li, R.H. Grubbs, D.A. Bansleben, M.W. Day, Organometallics 17 (1998) 3149;
(b) T.R. Younkin, E.F. Connor, J.I. Henderson, S.K. Friedrich, R.H. Grubbs, D.A. Bansleben, Science 287 (2000) 460.
[22] M.J. Rachita, R.L. Huff, J.L. Bennett, M. Brookhart, J. Polym. Sci. Polym. Chem. 38 (2000) 4627.
[23] D.L. Schroder, W. Keim, M.A. Zuideveld, S. Mecking, Macromolecules 35 (2002) 6071.
[24] (a) F.A. Hicks, M. Brookhart, Organometallics 20 (2001) 3217;
(b) J.C. Jenkins, M. Brookhart, Organometallics 22 (2003) 250.
[25] P. Braunstein, G. Clerc, X. Morise, R. Welter, G. Mantovani, Dalton Trans. (2003) 1601.
[26] R. Abeywickrema, M.A. Bennett, K.J. Cavell, M. Kony, A.F. Masters, A.G. Webb, J. Chem. Soc., Dalton Trans. (1993) 59.
[27] E.K. van den Beuken, W.J.J. Smeets, A.L. Spek, B.L. Feringa, Chem. Commun. (1998) 223.
[28] S.P. Meneghetti, P.J. Lutz, J. Kress, Organometallics 18 (1999) 2734.
[29] S. Tsuji, D.C. Swenson, R.F. Jordan, Organometallics 18 (1999) 4758.
[30] C. Carlini, M. Marchionna, A.M.R. Galletti, G. Sbrana, Appl. Catal. A 206 (2001) 1.
[31] M. Wang, X.M. Yu, Z. Shi, M.X. Qian, K. Jin, J.S. Chen, R. He, J. Organomet. Chem. 645 (2002) 127.
[32] (a) Z. Li, W.-H. Sun, Z. Ma, Y. Hu, C. Shao, Chin. Chem. Lett. 12 (2001) 691;
(b) C. Shao, W.-H. Sun, Z. Li, Y. Hu, L. Han, Catal. Commun. 3 (2002) 405;
(c) L. Wang, W.-H. Sun, L. Han, Z. Li, Y. Hu, C. He, C. Yan, J. Organomet. Chem. 650 (2002) 59;
(d) L. Wang, W.-H. Sun, L. Han, H. Yang, Y. Hu, X. Jin, J. Organomet. Chem. 658 (2002) 62;
(e) L. Chen, J. Hou, W.-H. Sun, Appl. Catal. A 246 (2003) 11.
[33] M.F. Elshazly, A. Eldissowky, T. Salem, M. Osman, Inorg. Chim. Acta 40 (1980) 1.
[34] K. Nakamoto, Infrared and Raman Spectra of Inorganic and Coordination Compounds, Part B, fifth ed., Wiley, New York, 1997, p. 183.
[35] M. Nonoyama, S. Tomita, K. Yamasaki, Inorg. Chim. Acta 12 (1975) 33.
[36] T.V. Laine, U. Piironen, K. Lappalainen, M. Klinga, E. Aitola, M. Leskela, J. Organomet. Chem. 606 (2000) 112.
[37] D. Guo, L. Han, T. Zhang, W.-H. Sun, T. Li, X. Yang, Macromol. Theory Simul. 11 (2002) 1006.
[38] W. Keim, J. Mol. Catal. 52 (1989) 19.
[39] K.A.O. Starzewski, J. Witte, Angew. Chem., Int. Ed. Engl. 24 (1985) 599.
[40] J. van Soolingen, H.D. Verkruijsse, M.A. Keegstra, L. Brandsma, Synth. Commun. 20 (1990) 3153.
[41] M. Hidai, T. Kashiwagi, T. Ikeuchi, Y. Uchida, J. Organomet. Chem. 30 (1971) 279.
[42] G.M. Sheldrick, SHELXTL-97, Program for the Refinement of Crystal Structures, University of Göttingen, Germany, 1997.
[43] SMART 5.0 and SAINT 4.0 for windows NT: area detector control and integration software, Bruker Analytical X-ray System, Inc., Madison, WI, 1998.
[44] G.M. Sheldrick, SADABS: Program for Empirical Absorption Correction of Area Detector Data, University of Göttingen, Germany, 1996.
[45] G.M. Sheldrick, SHELXTL: Structure Determination Software Program, Bruker Analytical X-ray System, Inc., Madison, WI, 1997.